

ห้องสมุดงานวิจัย สำนักงานคณะกรรมการวิจัยแห่งชาติ



E47266

STUDY OF LOCALIZATION IN SANDY SOIL
USING SHEAR WAVE LOGGING

MR. PULPONG PONGVITHAYAPANU

A DISSERTATION SUBMITTED IN PARTIAL FULFILLMENT OF THE REQUIREMENTS
FOR THE DEGREE OF DOCTOR OF PHILOSOPHY PROGRAM IN CIVIL ENGINEERING
DEPARTMENT OF CIVIL ENGINEERING
FACULTY OF ENGINEERING
CHULALONGKORN UNIVERSITY
ACADEMIC YEAR 2010
COPYRIGHT OF CHULALONGKORN UNIVERSITY

600254219



E47266

STUDY OF LOCALIZATION IN SANDY SOIL USING SHEAR WAVE LOGGING



Mr. Pulpong Pongvithayapanu

A Dissertation Submitted in Partial Fulfillment of the Requirements
for the Degree of Doctor of Philosophy Program in Civil Engineering
Department of Civil Engineering
Faculty of Engineering
Chulalongkorn University
Academic year 2010
Copyright of Chulalongkorn University



4 9 7 1 8 2 1 5 2 1

การศึกษาการวิบัติเฉพาะที่ของดินทรายด้วยคลื่นแรงเฉือน

นายพลพงษ์ พงษ์วิทยพานู

วิทยานิพนธ์นี้เป็นส่วนหนึ่งของการศึกษาตามหลักสูตรปริญญาวิศวกรรมศาสตรดุษฎีบัณฑิต

สาขาวิชาวิศวกรรมโยธา ภาควิชาวิศวกรรมโยธา

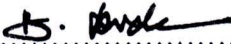
คณะวิศวกรรมศาสตร์ จุฬาลงกรณ์มหาวิทยาลัย

ปีการศึกษา 2553

ลิขสิทธิ์ของจุฬาลงกรณ์มหาวิทยาลัย

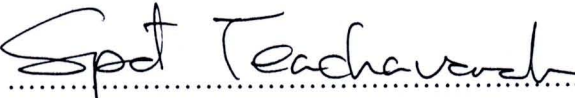
Thesis Title	STUDY OF LOCALIZATION IN SANDY SOIL USING SHEAR WAVE LOGGING
By	Mr. Pulpong Pongvithayapanu
Field of Study	Civil Engineering
Thesis Advisor	Associate Professor Supot Teachavorasinskun, D. Eng.

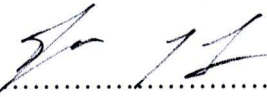
Accepted by the Faculty of Engineering, Chulalongkorn University in Partial
Fulfillment of the Requirements for the Doctoral Degree


.......... Dean of the Faculty of Engineering
(Associate Professor Boonsom Lerdhirunwong, Dr. Ing.)


THESIS COMMITTEE

.......... Chairman
(Assistant Professor Thavee Thanacharoengit, Dr. Ing.)

.......... Thesis Advisor
(Associate Professor Supot Teachavorasinskun, D. Eng.)

.......... Examiner
(Associate Professor Tirawat Boonyatee, D. Eng.)

.......... Examiner
(Associate Professor Suched Likitlersuang, D. Phil.)

.......... External Examiner
(Assistant Professor Siam Yimsiri, Ph. D.)

พลพจน์ พงษ์วิทย์ภานุ : การศึกษาการวิบัติเฉพาะที่ของดินทรายด้วยคลื่นแรงเฉือน.

(STUDY OF LOCALIZATION IN SANDY SOIL BY SHEAR WAVE LOGGING)

อ. ที่ปรึกษาวิทยานิพนธ์หลัก : รศ.ดร. สุพจน์ เตชวรสินสกุล, 140 หน้า.

E47266

การศึกษาการเกิดปรากฏการณ์ Localization ในมวลดินเป็นหัวข้อหนึ่งที่สำคัญในงานวิจัยทางวิศวกรรมปฐพีมากกว่า 50 ปี แม้ว่าการศึกษาวิจัยโดยอาศัยทฤษฎีและการจำลองทางคณิตศาสตร์จะสามารถทำให้ทราบถึงพฤติกรรม Localization ได้ดีในระดับหนึ่ง แต่เนื่องจากความไม่ต่อเนื่องของมวลดินภายในบริเวณดังกล่าวนี้มีความซับซ้อนมาก การศึกษาจากการทดสอบดินในห้องปฏิบัติการจะทำให้รู้ถึงพฤติกรรมของความไม่ต่อเนื่องดังกล่าวได้มากยิ่งขึ้น โดยอาศัยเครื่องมือทดสอบแบบดั้งเดิมและที่พัฒนาใหม่ เช่น การใช้รังสีแกมมา การใช้ภาพตัดขวางจากรังสีเอ็กซ์เรย์ และการวิเคราะห์ภาพถ่าย เป็นต้น แต่การทดสอบโดยใช้เครื่องมือดังกล่าว ผู้ทดสอบจำเป็นต้องมีความเชี่ยวชาญและประสบการณ์ด้านเทคนิคในการติดตั้งเครื่องมือ การใช้เครื่องมือ และการวิเคราะห์ผล ซึ่งในปัจจุบันการทดสอบโดยใช้ Bender Element ได้รับความนิยมอย่างแพร่หลายเนื่องจากความง่ายในการทดสอบและราคาไม่แพง การทดสอบโดยใช้ Bender Element นี้ส่วนใหญ่ใช้ในการวัดค่าความเร็วคลื่นแรงเฉือนเพื่อใช้คำนวณค่าโมดูลัสแรงเฉือนที่ระดับความเครียดต่ำ โดยตัวแปรหลายตัวที่มีผลกระทบต่อการเคลื่อนที่ของคลื่นแรงเฉือนผ่านตัวอย่างดินนี้มีผลกระทบต่อพฤติกรรมของการเกิด Localization ด้วยเช่นเดียวกัน เช่น ค่าอัตราส่วนช่องว่างและสถานะความเค้น เป็นต้น

ในงานวิจัยฉบับนี้จึงได้ทำการทดสอบตัวอย่างดินทรายห้องดินและทรายซิลิกาในเครื่องทดสอบแรงอัดสามแกนที่มีการติดตั้งอุปกรณ์ตัว Bender Element ไว้เพื่อทำการตรวจวัดคลื่นแรงเฉือนระหว่างการทดสอบตัวอย่าง เพื่อใช้ศึกษาพฤติกรรมในการเกิด Localization ในดิน โดยผลการทดสอบพบว่าเทคนิคการใช้คลื่นแรงเฉือนเพื่อดูพฤติกรรมการเกิดปรากฏการณ์ Localization นั้นสามารถอธิบายกระบวนการเกิดได้ดีในระดับหนึ่ง โดยความเร็วของคลื่นแรงเฉือนจะเริ่มลดลงจากค่าสูงสุด ณ ตำแหน่งความเครียดที่ประมาณ 0.5 – 3% ขึ้นอยู่กับสถานะความเค้นและค่าความหนาแน่นเริ่มต้นของตัวอย่างดินนั้น การลดลงของค่าความเร็วคลื่นแรงเฉือนนี้อธิบายได้ว่าเป็นจุดเริ่มต้นของการเกิดปรากฏการณ์ Localization ขึ้นในมวลดิน

ภาควิชาวิศวกรรมโยธา.... ลายมือชื่อนิสิต

สาขาวิชา.....วิศวกรรมโยธา.... ลายมือชื่อ อ.ที่ปรึกษาวิทยานิพนธ์หลัก

ปีการศึกษา2553.....

4971821521 : MAJOR CIVIL ENGINEERING

KEYWORDS : LOCALIZATION / BENDER ELEMENT / SHEAR WAVE

PULPONG PONGVITHAYAPANU : STUDY OF LOCALIZATION IN
SANDY SOIL USING SHEAR WAVE LOGGING. THESIS ADVISOR :
ASSOCIATE PROFESSOR SUPOT TEACHAVORASINSKUN, D.ENG,
140 pp.

E47266

Strain localization phenomenon in soils has been one of the main research topics in geotechnical engineering for more than 50 years ago. Though investigations by theoretical and numerical studies can expose some of the strain localization characteristics but are impeded because of the complexity inside that localized zones. On the other hand, the experimental studies can obviously investigate that particular behavior in more details. Both conventional and new apparatuses, i.e. Gamma-ray, X-ray Computed Tomography and Digital Image Analysis, have been adopted in the strain localization analyses. However, those techniques require technical proficiency and experience in the installation, operation and result interpretation. The bender element test nowadays is becoming quite popular in geotechnical engineering because of its simplicity, relatively low cost and nondestructive test. A pair of bender elements has been extensively used to measure shear wave velocity for the determination of small strain shear modulus inside the soil sample. This shear wave propagation throughout the soil specimen influences in the same way by several of the same factors, e.g. void ratio and state of stress, compared to localization mechanism.

A series of compression triaxial tests implemented by bender element installation was performed to investigate the occurrence of strain localization in sand of various types, i.e. local and Silica sand. The results showed that this shear wave propagation technique can describe to some extent some characteristics of localization mechanism. The shear wave velocity tends to decrease from its maximum value at a certain strain level, i.e. 0.5 - 3% of global axial strain, depending on the state of stress as well as the initial packing condition of the sample. This diminution of shear wave velocity is the initiation of soil non-uniformity deformation or the onset of strain localization inside the sand specimen.

Department : Civil Engineering

Field of Study : Civil Engineering

Academic Year : 2010

Student's Signature

Advisor's Signature

ACKNOWLEDGEMENTS

This research was motivated, supervised and strongly supported by my advisor Associate Professor Supot Teachavorasinskun. His insight, encouragement, dedication, and great personality helped me throughout this research. This dissertation is the product of his guidance and encouragement. He is the first and the best teacher who enlightens me to conduct researches in geotechnical and earthquake engineering.

The dissertation committee has also played an important role in the completion of this thesis. I am indebted to Associate Professor Tirawat Boonyatee for providing me some testing apparatuses as well as giving me valuable guidance. I want to thank Assistant Professor Siam Yimsiri and Associate Professor Suched Likitlersuang for his constructive criticism of this work and for his advice on academic matters. Finally, I am grateful to Assistant Professor Thavee Thanacharoengit for serving as chair of the dissertation committee.

I gratefully acknowledge the financial support provided by the Commission on Higher Education, Ministry of Education under Faculty Development Scholarship Program with the collaboration of AUN/SEED-Net. I also would like to express my deepest gratitude to Professor Masayuki Hyodo for having accepted me as a foreign researcher at the geotechnical engineering laboratory, Yamaguchi University, Ube, Japan.

Special thanks for my colleague, Mr. Montree Masgul for his helps in all tests and valuable discussions.

Finally, I want to thank the most important people in my life. My parents have been a constant source of encouragement ever since I was a child. My parents were my first teachers; they taught me the most important things in life. My wife Pataranee has been my one's beloved for ten years and forever. I would like to express my love and gratitude for her understanding and endless love. I also thank to Mrs. Sutanee Kajudphai for her inexhaustible supports all the time.

CONTENTS

	Page
ABSTRACT (IN ENGLISH)	iv
ABSTRACT (IN THAI)	v
ACKNOWLEDGEMENTS	vi
CONTENTS	vii
LIST OF TABLES	ix
LIST OF FIGURES	x
LIST OF SYMBOLS	xix
CHAPTER	
I Introduction	
1.1 Introduction	1
1.2 Objective of the Study	3
1.3 Scope of the Study	3
II Literature Review	
2.1 Strain Localization in Granular Soils.....	5
2.1.1 Theoretical and numerical approach	6
2.1.2 Experimental approach	12
2.2 Factor Affecting Strain Localization	28
2.2.1 Mean effective stress and confining stress	29
2.2.2 Loading conditions	31
2.2.3 Specimen geometry	33
2.2.4 Grain size	35
2.2.5 Role of imperfection	35
2.3 Bender Element Test and Shear Wave Velocity in Particulate Materials	37
2.3.1 Bender element	37
2.3.2 Travel time determination	39
2.3.3 Potential problems in bender element testing	44

CHAPTER	Page
III Methodology	
3.1 Material Properties	48
3.2 Sample Preparation.....	48
3.3 Bender Element	51
3.4 Digital Image Analysis (DIA)	53
3.5 Triaxial Compression Test by Vacuum Technique	53
3.6 Experimental Works	55
3.7 Calculation of Travel Time and Shear Wave Velocity.....	57
IV Results and Analyses	
4.1 The Stress Strain Responses from Triaxial Tests	63
4.2 Shear Wave Velocity During Isotropic Loading and Shearing	68
4.2.1 Shear wave velocity under isotropic loading	68
4.2.2 Shear wave velocity during shear	72
4.3 The Initiation and Persistent of Strain Localization	79
4.3.1 Observation from shear wave velocity profile and stress ratio	79
4.3.2 Observation from Digital Image Analysis (DIA) technique	94
V Conclusions and Recommendations	
5.1 Conclusions	107
5.2 Recommendations for Future Research.....	108
REFERENCES	109
BIOGRAPHY	121

LIST OF TABLES

	Page
Table 3.1 The basic engineering properties of sand samples	50
Table 3.2 Qualitative description of granular soil deposits	51
Table 3.3 All testing conditions and specimen properties of this study	58
Table 4.1 Summary of the test results of stress - strain relationship	67

LIST OF FIGURES

	Page
Figure 2.1 Mohr's stress circles and strength envelopes for cast iron	4
Figure 2.2 Mohr-Coulomb solution to shear orientation	7
Figure 2.3 Roscoe solution to shear band orientation.....	8
Figure 2.4 Plane strain compression apparatus	14
Figure 2.5 Formation of shear zone in dense specimen.....	15
Figure 2.6 Schematic diagram of a plane strain apparatus at the University of Grenoble	16
Figure 2.7 Evolution of the stress ratio and void ratio and formation of a shear zone during the experiment with a high dense specimen and non-lubricated ends.....	17
Figure 2.8 Evolution of the stress ratio and void ratio formation of shear zones during the experiment with a low dense specimen and lubricated ends	18
Figure 2.9 X-ray photography used on plane strain models allowed Roscoe and his collaborators to show the large dilatancy taking place in shear zones in retaining wall models.....	19
Figure 2.10 Stereophotogrammetry-based incremental fields of shear strain intensity and volumetric strain	20
Figure 2.11 Gamma-ray device used to measure the local density in shear bands in plane strain specimens.....	21
Figure 2.12 Density profile across a shear band in plane strain test of dense specimen with low confining pressure recorded by Gamma-ray absorption	21
Figure 2.13 Density profile before and after loading in plane strain test of dense specimen with low confining pressure	22
Figure 2.14 Experimental device: specimen, triaxial cell, scanner field measurement and reaction frame and the technique of CT scan .	22

	Page
Figure 2.15 CT scan technique of two orthogonal axial sections and two cross sections taken at one third and two thirds of the specimens height under conventional triaxial compression experiments with various test conditions.....	24
Figure 2.16 Schematic of experiment apparatus to study strain localization by DIA	25
Figure 2.17 Specimen image (a) before compression (axial strain = 0 %) (b) deformed specimen at 3.8% axial strain (c) magnified image showing grid relative displacement within shear band.....	25
Figure 2.18 Schematic of cross section of specimen resin impregnation setup and typical microscopic image of the tested sand after hardening in the epoxy	26
Figure 2.19 Strain localization using DIA techniques	27
Figure 2.20 An example of contour plots and the digital image of shear band formation.....	27
Figure 2.21 DIC measured displacements surrounding a persistent shear band	28
Figure 2.22 Stress strain responses from four tests on dense RF Hostun sand	29
Figure 2.23 Stress strain responses from four tests on loose RF Hostun sand	30
Figure 2.24 Principal stress ratio versus axial strain and volumetric strain versus axial strain for CTC	31
Figure 2.25 Stress-strain relationship for plane strain and triaxial specimens	32
Figure 2.26 Comparison between CTC and PS experiments of dense specimens	33
Figure 2.27 Trace of the single shear plane in long specimen of Triaxial test on sand	34
Figure 2.28 Two cross-sections recorded in a short specimen, revealing complex localization patterns	34
Figure 2.29 Stereophotogrammetry-based incremental fields of shear strain intensity	36

	Page
Figure 2.30 Reconstruction of void ratio field in an axial tomogram of sand specimen	37
Figure 2.31 Bender elements	38
Figure 2.32 Bender element types and connections	38
Figure 2.33 Schematic of bender element system	39
Figure 2.34 Schematic representation of the conventional travel time measurement for shear wave velocity calculation	40
Figure 2.35 Input pulse of shear wave	41
Figure 2.36 First time of arrival and the time between first peak to peak	41
Figure 2.37 The time of arrival using cross-correlation method	43
Figure 2.38 (a) Representation of the lock-in amplifier as a tuneable filter (b) representation of the output of the dual-phase lock-in amplifier as a vector	44
Figure 2.39 Near-field effect of received shear wave signals at different frequencies	45
Figure 2.40 Crosstalk effects	46
Figure 3.1 Shape of grain particles	49
Figure 3.2 The photo effect of grain particles.....	49
Figure 3.3 The installation of parallel- or series-type of bender element in the top / bottom cap of the triaxial apparatus	52
Figure 3.4 The printed square grid on the rubber membrane surface of the specimens.....	54
Figure 3.5 The schematic view of triaxial testing by vacuum technique.....	54
Figure 3.6 The schematic view of the bender element test setup incorporated in a triaxial cell apparatus.....	55
Figure 3.7 The graphical display of typical transmitter and receiver wave from oscilloscope processing	56
Figure 3.8 The schematic chart of all testing procedures	59
Figure 3.9 Typical S-wave signal within near field	60

	Page
Figure 3.10 The interpretation method to point out the first arrival time of shear wave justified for the near field effect and reflecting <i>P</i> -waves	61
Figure 3.11 The effect of near field and reflecting <i>P</i> -wave of the receiver signal	62
Figure 4.1 The stress - strain relation of D16 specimen in loose and dense conditions with confining pressure 80, 50 and 25 kPa	64
Figure 4.2 The stress - strain relation of D40 specimen in loose and dense conditions with confining pressure 80, 50 and 25 kPa	65
Figure 4.3 The stress - strain relation of Silica specimen in loose and dense conditions with confining pressure 80, 50 and 25 kPa	66
Figure 4.4 The shear wave velocity and stress relation of D16 sand in loose and dense conditions and its empirical relation	69
Figure 4.5 The shear wave velocity and stress relation of D40 sand in loose and dense conditions and its empirical relation	69
Figure 4.6 The shear wave velocity and stress relation of Silica sand in loose and dense conditions and its empirical relation	70
Figure 4.7 Typical values for α and β coefficients	70
Figure 4.8 The variation between shear wave velocity and void ratio of D16, D40 and Silica sand in loose and dense conditions under isotropic loading	72
Figure 4.9 The influence of mean effective stress to the shear wave velocity on D16 for a) loose and b) dense state in various confining conditions	75
Figure 4.10 The influence of mean effective stress to the shear wave velocity on D40 for a) loose and b) dense state in various confining conditions	75
Figure 4.11 The influence of mean effective stress to the shear wave velocity on Silica test sand for a) loose and b) dense state in various confining conditions	75

	Page
Figure 4.12 The influence of deviator stress to the shear wave velocity on D16 for a) loose and b) dense state in various confining conditions.....	76
Figure 4.13 The influence of deviator stress to the shear wave velocity on D40 for a) loose and b) dense state in various confining conditions.....	76
Figure 4.14 The influence of deviator stress to the shear wave velocity on Silica test sand for a) loose and b) dense state in various confining conditions	76
Figure 4.15 The variation between the shear wave velocity and the principal stress ratio on D16 for a) loose and b) dense state in various confining conditions	77
Figure 4.16 The variation between the shear wave velocity and the principal stress ratio on D40 for a) loose and b) dense state in various confining conditions	77
Figure 4.17 The variation between the shear wave velocity and the principal stress ratio on Silica test sand for a) loose and b) dense state in various confining conditions	77
Figure 4.18 Shear wave propagation during isotropic consolidation and shear	78
Figure 4.19 The effective stress ratio vs global axial strain of biaxial test in sand and the stereophotogrammetry-based increment fields of shear strain intensity	79
Figure 4.20 (a) The lateral deformation measurement (b) the lateral strain vs the global axial strain at two elevations (c) the absolute width difference between the upper and lower parts of the specimen and the sled or block movement	80
Figure 4.21 Evolution of shear bands (a) images from intervals of global axial strain by stereo-comparison (b) axial load curve.....	81

	Page
Figure 4.22 Stress strain response in terms of stress ratio during shear	82
Figure 4.23 The stress ratio and shear wave velocity (V_s) against strain for D16 in loose condition with confining pressure 80 kPa	84
Figure 4.24 The stress ratio and shear wave velocity (V_s) against strain for D16 in loose condition with confining pressure 50 kPa	84
Figure 4.25 The stress ratio and shear wave velocity (V_s) against strain for D16 in loose condition with confining pressure 25 kPa	85
Figure 4.26 The stress ratio and shear wave velocity (V_s) against strain for D16 in dense condition with confining pressure 80 kPa.....	85
Figure 4.27 The stress ratio and shear wave velocity (V_s) against strain for D16 in dense condition with confining pressure 50 kPa.....	86
Figure 4.28 The stress ratio and shear wave velocity (V_s) against strain for D16 in dense condition with confining pressure 25 kPa.....	86
Figure 4.29 The stress ratio and shear wave velocity (V_s) against strain for D40 in loose condition with confining pressure 80 kPa	87
Figure 4.30 The stress ratio and shear wave velocity (V_s) against strain for D40 in loose condition with confining pressure 50 kPa	87
Figure 4.31 The stress ratio and shear wave velocity (V_s) against strain for D40 in loose condition with confining pressure 25 kPa	88
Figure 4.32 The stress ratio and shear wave velocity (V_s) against strain for D40 in dense condition with confining pressure 80 kPa.....	88
Figure 4.33 The stress ratio and shear wave velocity (V_s) against strain for D40 in dense condition with confining pressure 50 kPa.....	89
Figure 4.34 The stress ratio and shear wave velocity (V_s) against strain for D40 in dense condition with confining pressure 25 kPa.....	89
Figure 4.35 The stress ratio and shear wave velocity (V_s) against strain for Silica sand in loose condition with confining pressure 80 kPa ...	90
Figure 4.36 The stress ratio and shear wave velocity (V_s) against strain for Silica sand in loose condition with confining pressure 50 kPa ...	90

	Page
Figure 4.37 The stress ratio and shear wave velocity (V_s) against strain for Silica sand in loose condition with confining pressure 25 kPa ...	91
Figure 4.38 The stress ratio and shear wave velocity (V_s) against strain for Silica sand in dense condition with confining pressure 80 kPa...	91
Figure 4.39 The stress ratio and shear wave velocity (V_s) against strain for Silica sand in dense condition with confining pressure 50 kPa...	92
Figure 4.40 The stress ratio and shear wave velocity (V_s) against strain for Silica sand in dense condition with confining pressure 25 kPa...	92
Figure 4.41 The typical results of stress-strain and the profile of V_s propagation inside sample during the compression test	93
Figure 4.42 Evolution of local axial strain profile during axial compression loading of D16 sample in loose condition with confining pressure 25 kPa	95
Figure 4.43 (a) Failure specimen and selected local elements (b) relationship Between local and global axial strain (c) stress ratio of the highest deformed element of D16 sample in loose condition with confining pressure 25 kPa	95
Figure 4.44 Evolution of local axial strain profile during axial compression loading of D16 sample in dense condition with confining pressure 25 kPa	96
Figure 4.45 (a) Failure specimen and selected local elements (b) relationship Between local and global axial strain (c) stress ratio of the highest deformed element of D16 sample in dense condition with confining pressure 25 kPa	96
Figure 4.46 Evolution of local axial strain profile during axial compression loading of D16 sample in loose condition with confining pressure 80 kPa	97
Figure 4.47 (a) Failure specimen and selected local elements (b) relationship Between local and global axial strain (c) stress ratio of the highest deformed element of D16 sample in loose condition with confining pressure 80 kPa	97

	Page
Figure 4.48 Evolution of local axial strain profile during axial compression loading of D16 sample in dense condition with confining pressure 80 kPa	98
Figure 4.49 (a) Failure specimen and selected local elements (b) relationship Between local and global axial strain (c) stress ratio of the highest deformed element of D16 sample in dense condition with confining pressure 80 kPa	98
Figure 4.50 Evolution of local axial strain profile during axial compression loading of Silica sample in loose condition with confining pressure 80 kPa	99
Figure 4.51 (a) Failure specimen and selected local elements (b) relationship Between local and global axial strain (c) stress ratio of the highest deformed element of Silica sample in loose condition with confining pressure 80 kPa	99
Figure 4.52 Evolution of local axial strain profile during axial compression loading of Silica sample in dense condition with confining pressure 80 kPa	100
Figure 4.53 (a) Failure specimen and selected local elements (b) relationship Between local and global axial strain (c) stress ratio of the highest deformed element of Silica sample in dense condition with confining pressure 80 kPa	100
Figure 4.54 The stress ratio, shear wave velocity and local strain profile of D16 sample in loose condition with confining pressure 25 kPa .	104
Figure 4.55 The stress ratio, shear wave velocity and local strain profile of D16 sample in dense condition with confining pressure 25 kPa	104
Figure 4.56 The stress ratio, shear wave velocity and local strain profile of D16 sample in loose condition with confining pressure 80 kPa..	105
Figure 4.57 The stress ratio, shear wave velocity and local strain profile of D16 sample in dense condition with confining pressure 80 kPa.	105

	Page
Figure 4.58 The stress ratio, shear wave velocity and local strain profile of Silica sample in loose condition with confining pressure 80 kPa	106
Figure 4.59 The stress ratio, shear wave velocity and local strain profile of Silica sample in dense condition with confining pressure 80 kPa	106

LIST OF SYMBOLS

V_s	shear wave velocity
σ_c	failure stress in compression
σ_t	failure stress in tension
τ_{ult}	failure stress in pure shear
τ_f	shear strength per unit area
c	cohesion
σ_n	normal stress
ϕ	angle of shearing resistance
σ_c	normal stress at failure
τ_c	shear stress at failure
θ_c	angle between the major principal stress direction and shear band
θ_R	inclination angle between shear band and the major principal strain increment direction
θ_A	inclination angle of the shear bands which include the effects of friction angle and angle of dilatancy.
σ_1	major principle stress
σ_3	minor principle stress
$d\varepsilon_1$	major principal strain increment
$d\varepsilon_3$	minor principal strain increment
ψ	angle of dilatancy
d_{50}	mean grain size
U	uniformity coefficient
ρ_d	dry density
γ_d^{max}	maximum specific weight
γ_d^{min}	minimum specific weight
e	void ratio

e_{min}	minimum void ratio
e_{max}	maximum void ratio
D_r	relative density
G_s	specific gravity
t/s'	stress ratio
ε_v	volumetric strain
ε_1	axial strain
ε_a	global axial strain
G_{max}	small strain stiffness
L, L_{tr}	tip-to-tip distance between transmitter and receiver of bender element
t	travel time of the shear wave from transmitter to receiver
t_0	first time of arrival
t_{pp}	time between first peak to peak
t_{cc}, τ	time shift
$CC_{yx}(t)$	cross-correlation function
T	total duration of the time record
dt	change in time-of-flight in seconds
$d\theta$	change in phase angle in degrees
f	frequency of the driving wave in Hertz
L_u	wave path length
λ	wavelength
H/D	slenderness ratio
σ'_c	confining pressure
q'	deviator stress
σ'_1	effective stress in the direction of shear wave propagation
σ'_3	effective stress in the direction of particle motion
σ'_{mean}	mean state of stress
σ'_0	isotropic loading

- α, β parameters include contact effects, void ratio, coordination number, fabric change and the loading history
- A effect of grain properties
- $F(e)$ influence of packing properties
- C_n coordination number
- Ω, Θ void ratio of the arrangement at constant fabric as well as the packing property
- $\theta, \delta, \zeta, \psi$ contact effect and the influence of fabric change
- Ψ effect of void ratio
- φ exponent parameter reflecting the contact behavior under anisotropic loading
- q'/p' principal stress ratio